

ACKNOWLEDGMENTS

I am very thankful for the hospitality shown me at the Kellogg Radiation Laboratory, discussions with Professor W. A. Fowler and Professor T. Lauritsen and experimental assistance during various phases of this

work by Dr. J. B. Marion, Mr. R. E. Pixley, and Mr. W. Zimmerman, Jr. A grant from the Swedish Atomic Committee and a Fulbright Fellowship are gratefully acknowledged. Professor K. Clusius, Zürich, kindly presented the enriched $O^{17}O^{18}$ gas.

Optical-Model Analysis of the Elastic Scattering of Alpha Particles*

G. IGO† AND R. M. THALER

Los Alamos Scientific Laboratory, University of California, Los Alamos, New Mexico

(Received December 26, 1956)

The elastic scattering of 22- and 40-Mev alpha particles on a variety of elements has been analyzed in terms of an optical model. The nuclear optical model potential assumed in this work has the form: $(V_R + iV_i)/\{1 + \exp[(r - r_1)/d]\}$. The diffuse character of the electrical charge distribution in nuclei was also taken into account. The four parameters in the nuclear optical model potential were varied so as to obtain the best fit to the data. The diffuseness parameter is found to be $d \approx 0.5 \times 10^{-13}$ cm and the parameter r_1 , which represents an "average" radius of the nucleus-alpha particle system, is found to be $r_1 \approx (1.35A^{1/3} + 1.3) \times 10^{-13}$ cm. The average values of V_R and V_i are -45 Mev and -10 Mev, respectively, at 40 Mev. Exceptions to this are the lightest elements, C, Al, and Ti, which require -30 Mev for V_R . At 22 Mev, V_R is found to be -31 Mev. Other parameters have the same values obtained at 40 Mev.

I. INTRODUCTION

DURING the past few years, there has been a steady increase in the information available concerning the elastic scattering of various particles from nuclei in the 10–50 Mev energy range. The proton and neutron elastic-scattering data have been analyzed in terms of an optical model.¹ The results of the proton analysis² indicate that the interaction potential must have a sloping edge in order to fit the small cross section, observed at large scattering angles. The nuclear potential considered by Saxon and Woods has the form $(V_R + iV_i)/\{1 + \exp[(r - r_1)/d]\}$. The parameter d is found to be approximately 0.5×10^{-13} cm, and when r_1 is taken to be $1.4A^{1/3} \times 10^{-13}$ cm, V_R is found to be approximately -39 Mev and V_i to be -10 Mev. However, recent work has indicated that equally good fits can be obtained with a radius of $1.20A^{1/3} \times 10^{-13}$ cm with $V_R \sim -60$ Mev.³

The qualitative features of the alpha-particle data suggest the possibility of fitting these data through the use of an optical-model potential. The success of similar calculations for nucleon-nucleus scattering encourages such a point of view. While it is *a priori* not so clear for alpha-particle scattering as for nuclear scattering that this model should apply, there is the advantage afforded in the alpha-particle analysis that the bombarding par-

ticle has zero spin. Thus, unlike the optical-model analysis of nucleon-nucleus scattering, no uncertainty arises from the possibility that a spin-orbit force plays an important role.⁴

Analyses of alpha-particle elastic scattering data from heavy elements only have been made by Porter,⁵ by Blair,⁶ by Wall *et al.*,⁷ and by Oda and Harada.⁸ Porter used a classical model which took into account the nuclear absorption of alpha particles in the surface. Blair employed a partial-wave analysis in which it was assumed that all partial waves which have classical impact parameters less than or equal to the interaction radius were totally absorbed. Wall *et al.* performed the same analysis on their data but assumed that the partial waves with classical impact parameters approximately equal to the interaction radius were only partially absorbed. Oda and Harada use the boundary condition model of Feshbach and Weisskopf⁹ and the optical model with a complex potential of exponential shape. These analyses were not successful in reproducing the elastic scattering data where the differential cross section deviated markedly from the Coulomb cross section. Three of these analyses^{6–8} compelled the use of an anomalously large radius for the alpha-particle-nucleus system.

⁴ W. B. Riesenfeld and K. M. Watson, *Phys. Rev.* **102**, 1157 (1956). G. Takeda and K. M. Watson, *Phys. Rev.* **94**, 1087 (1954); **97**, 1336 (1955).

⁵ C. E. Porter, *Phys. Rev.* **99**, 1400 (1955).

⁶ J. S. Blair, *Phys. Rev.* **95**, 1218 (1954).

⁷ Wall, Rees, and Ford, *Phys. Rev.* **97**, 726 (1955).

⁸ N. Oda and K. Harada, *Progr. Theoret. Phys. (Japan)* **15**, 545 (1956).

⁹ See for instance: J. M. Blatt and V. F. Weisskopf, *Theoretical Nuclear Physics* (John Wiley and Sons, Inc., New York, 1952).

* Work performed under the auspices of the U. S. Atomic Energy Commission.

† Permanent address: Stanford University, Stanford, California.

¹ See, for instance, "Statistical Aspects of the Compound Nucleus," Brookhaven National Laboratory Report BNL-331, 1955 (unpublished).

² R. D. Woods and D. S. Saxon, *Phys. Rev.* **95**, 577 (1954).

³ M. A. Melkanoff (private communication).

Two recent papers present values for the depth of the nuclear potential for alpha particles. Recently Mohr and Robson¹⁰ analyzed the 22-Mev elastic alpha-particle scattering data⁷ from Ag and Pb. They find that the Ag data requires a rounded potential such as was used by Woods and Saxon² with V_R between 0 and -62 Mev and $V_i = -62$ Mev, while for Pb, a square well with $V_R = 0$ and $V_i = -62$ Mev was adequate. Born-approximation phase shifts were used in this work. Tolhoek and Brussard¹¹ have used a very deep potential to fit the alpha disintegration data.

In this paper, the 40- and 22-Mev alpha-particle elastic scattering data are interpreted in terms of the optical model. It is assumed that the potential is a diffuse potential of the form employed by Saxon and Woods. Account is also taken of the distribution of charge in the nucleus.

II. THE OPTICAL MODEL

The scattering of an alpha particle of finite size by a nucleus is treated as the scattering of a point charge from a potential. This potential consists of a nuclear optical model part plus a Coulomb part. The Coulomb potential is assumed to be that from a fictitious radial charge distribution which approximately takes into account the finite extent of the charge distributions of both the bombarding and target nucleus.

In this approximation the Schrödinger equation to be solved for the l th partial wave may be written as

$$\frac{\hbar^2}{2\mu} \frac{d^2 U_l}{dr^2} = \left[V_{\text{nuc}} + V_{\text{coul}} + \frac{\hbar^2 l(l+1)}{2\mu r^2} - E_{\text{c.m.}} \right] U_l, \quad (1)$$

where μ is the reduced mass and $E_{\text{c.m.}}$ is the energy in the center-of-mass system. The Coulomb potential

energy is chosen to be that due to a radial charge distribution of the form¹²

$$\rho(r) \sim 1 - \frac{1}{2} \exp[n(r/r_0 - 1)], \quad r \leq r_0 \\ \sim \frac{1}{2} \exp[n(1 - r/r_0)], \quad r \geq r_0. \quad (2)$$

The Coulomb potential energy due to such a charge distribution is given in reference 12, as

$$V_{\text{coul}} = \frac{Z_1 Z_2 e^2}{r_0} \left[\frac{1}{n^2} + \frac{1}{2} \frac{x^2}{6} + \frac{e^{-n}}{n^2} \left(\frac{1 - e^{nx}}{nx} + \frac{1}{2} e^{nx} \right) \right] / \\ \left(\frac{1}{3} + \frac{2}{n^2} + \frac{e^{-n}}{n^3} \right), \quad x \leq 1 \\ = \frac{Z_1 Z_2 e^2}{r_0} \left[\frac{1}{x} - e^{n-nx} \left(\frac{1}{x} + \frac{n}{2} \right) \right] / \\ \left(e^{-n} + 2n + \frac{n^3}{3} \right), \quad x \geq 1, \quad (3)$$

where $x \equiv r/r_0$. The nuclear optical-model potential is assumed to be of the form:

$$V_{\text{nuc}} = (V_R + iV_i) / \{1 + \exp[(r - r_1)/d]\}, \quad (4)$$

where d is the diffuseness parameter and r_1 is the nuclear radius parameter. In the present work the assumption has been made that $r_0 = 1.30A^{1/3} \times 10^{-13}$ cm for heavy elements and $1.22A^{1/3} \times 10^{-13}$ cm for Ti, Al, and C. These

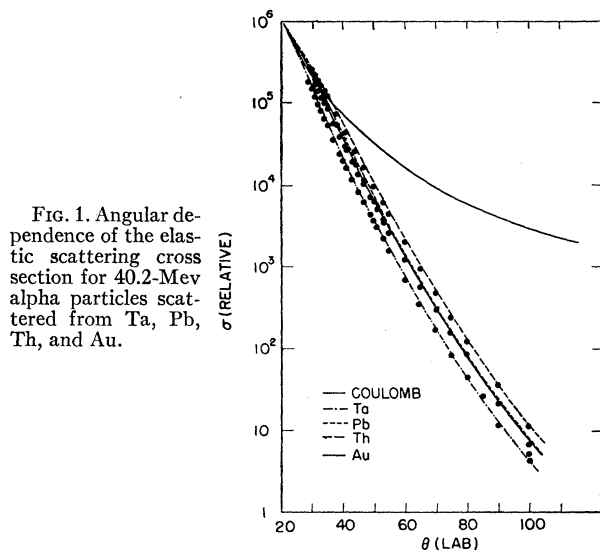


FIG. 1. Angular dependence of the elastic scattering cross section for 40.2-Mev alpha particles scattered from Ta, Pb, Th, and Au.

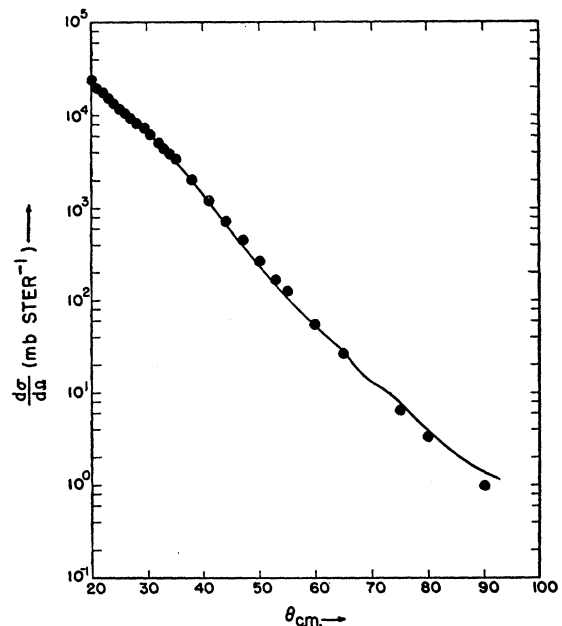


FIG. 2. Angular dependence of the elastic scattering cross section for 40.2-Mev alpha particles scattered from Th. The dots represent the experimental points; the solid line represents the theoretically predicted distribution for $V_R = -50$ Mev and $V_i = -7.5$ Mev.

¹⁰ C. B. O. Mohr and R. H. Robson, Proc. Phys. Soc. (London) A69, 365 (1956).

¹¹ H. A. Tolhoek and P. J. Brussard, Physica 21, 449 (1955).

¹² D. L. Hill and K. W. Ford, Phys. Rev. 94, 1617 (1954).

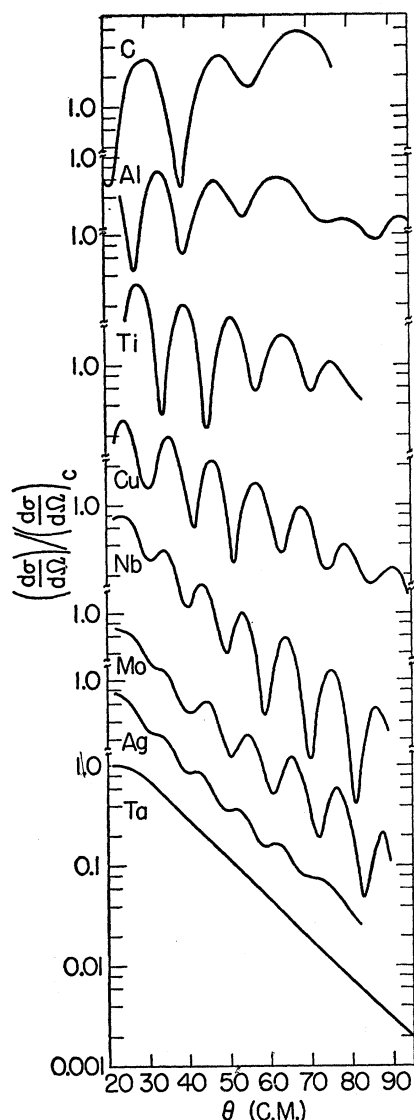


FIG. 3. The experimental ratio of the elastic scattering cross section to the pure Coulomb cross section for 40.2-Mev alpha particles scattered from various elements.

TABLE I. Optical model potential parameters for alpha-particle scattering on various elements. The potential is of the form $(V_R + iV_i) / \{1 + \exp[(r - r_i)/d]\}$. The parameters V_R and V_i are given in the table, with $r_i = (1.35A^{1/3} + 1.3) \times 10^{-13}$ cm and $d = 0.5 \times 10^{-13}$ cm.

E (Mev)	Element	$-V_R$ (Mev)	$-V_i$ (Mev)
40.2	C	30	10
40.2	Al	30	12
40.2	Ti	30	14
40.2	Cu	46.8	13
40.2	Nb	45	13.5
40.2	Mo	42	9.5
40.2	Ag	37	10
40.2	Ta	51	9
40.2	Au	44	10
40.2	Pb	43	7.6
40.2	Th	50	7.5
20	Ag	35	7.5
20	Au	30	9.5
20	Pb	30	16

values were chosen rather than the smaller value obtained from the Stanford electron scattering experiments¹³ since the charge distribution is probably broadened by the alpha-particle charge distribution. The differential equation [Eq. (1)] was numerically integrated by the method proposed by Gill.¹⁴ The solutions so obtained were compared with the Coulomb wave functions.¹⁵ The complex phase shifts δ_l are given by

$$\delta_l = -\tan^{-1} \left| \frac{(F_l'/G_l) - (U_l'/U_l)}{(F_l'/G_l) + (U_l'/U_l)} \right|, \quad (5)$$

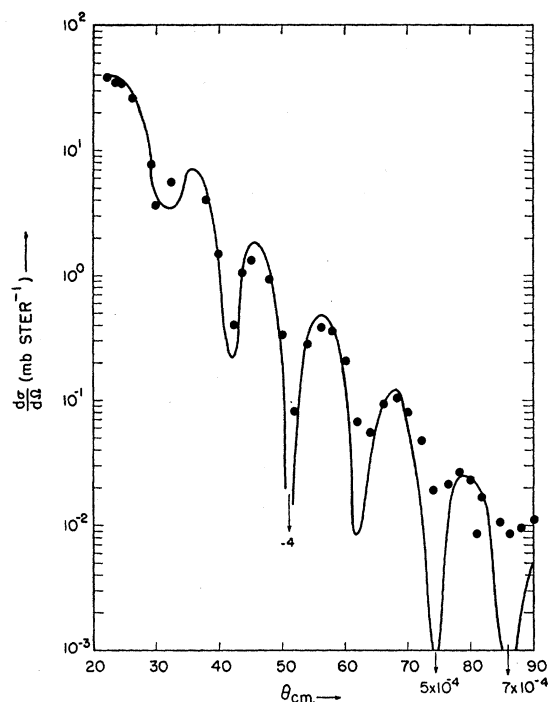


FIG. 4. Angular dependence of the elastic scattering cross section for 40.2-Mev alpha particles scattered from Cu. The dots represent the experimental points; the solid line represents the theoretically predicted distribution for $V_R = -49.5$ Mev and $V_i = -11$ Mev.

where F_l , G_l are the regular and irregular Coulomb functions, respectively, and the primes represent derivatives of the indicated quantities. The differential cross section for elastic scattering is given by

$$\sigma_{el}(\theta) = \frac{1}{k^2} \left| \frac{\eta \exp\{-i\eta \ln[\sin^2(\theta/2)]\}}{2\sin^2(\theta/2)} + \frac{1}{2i} \sum_{l=0}^{\infty} (2l+1) e^{2i(\sigma_l - \sigma_0)} [e^{2i\delta_l} - 1] P_l(\cos\theta) \right|^2 \quad (6)$$

¹³ Yennie, Ravenhall, and Wilson, Phys. Rev. **95**, 500 (1954).

¹⁴ S. Gill, Proc. Cambridge Phil. Soc. **47**, 96 (1951).

¹⁵ The method of calculation for the Coulomb wave functions is discussed by R. M. Thaler and L. C. Biedenharn, Nuclear Phys. (to be published).

where

$$\eta \equiv (Z_1 Z_2 e^2 / h v_{rel}), \quad \sigma_l \equiv \arg \Gamma(l+1+i\eta),$$

and P_l is the Legendre polynomial. At an energy of 40 Mev it proved necessary to consider twenty-five to thirty partial waves. At 22 Mev fifteen to twenty partial waves sufficed.

III. ANALYSIS OF ELASTIC SCATTERING DATA

The elastic scattering of alpha particles from Th at 40.2 Mev is typical of the heavy-element data¹⁶ at that energy which are summarized in Fig. 1. The differential cross section at small angles is equal to the Coulomb cross section, rises above the Coulomb cross section at

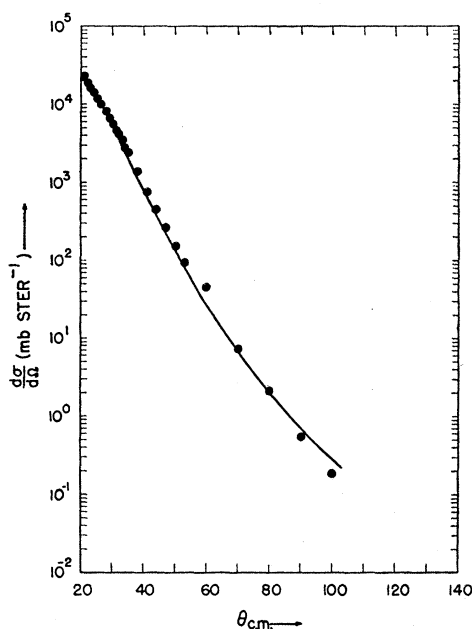


FIG. 5. Angular dependence of the elastic scattering cross section for 40.2-Mev alpha particles scattered from Pb. The dots represent the experimental points; the solid line represents the theoretically predicted distribution for $V_R = -43$ Mev and $V_i = -7.6$ Mev.

some critical angle, and then drops monotonically to about 1/1000 the Coulomb differential cross section at the largest angle of measurement.

The best fit (Fig. 2) to the experimental data at 40.2 Mev was obtained when the interaction radius was taken to be $R = 9.6 \times 10^{-13}$ cm = $(1.35A^{1/3} + 1.3) \times 10^{-13}$ cm. The quantities V_R and V_i were allowed to vary between 0 and -100 Mev in a grid with a 10-Mev spacing. A larger radius was tried, namely, $R = 11.4 \times 10^{-13}$ cm = $(1.5A^{1/3} + 2.2) \times 10^{-13}$ cm, a value obtained in an earlier analysis.⁶ The quantities V_R and V_i were allowed to vary within the same limits again. The best fit obtained for the latter case had a least-square deviation several hundred times larger than for the former.

¹⁶ Wegner, Eisberg, and Igo, Phys. Rev. 99, 825 (1955).

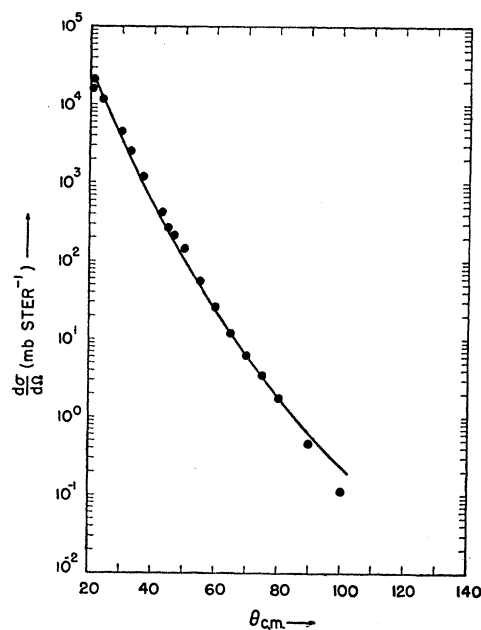


FIG. 6. Angular dependence of the elastic scattering cross section for 40.2-Mev alpha particles scattered from Au. The dots represent the experimental points; the solid line represents the theoretically predicted distribution for $V_R = -44$ Mev and $V_i = -10$ Mev.

With the radius taken to be 9.59×10^{-13} cm, the parameter d was varied from 1.0 to 0.25×10^{-13} cm. The best fit for $d = 1.0$ occurred for $V_R \sim 0$ and for V_i very

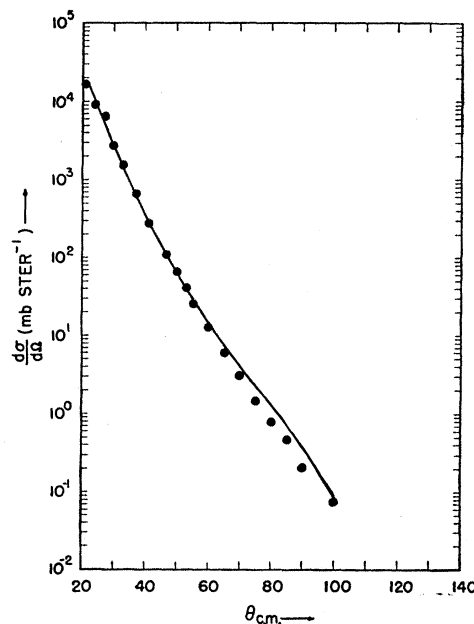


FIG. 7. Angular dependence of the elastic scattering cross section for 40.2-Mev alpha particles scattered from Ta. The dots represent the experimental points; the solid line represents the theoretically predicted distribution for $V_R = -51$ Mev and $V_i = -9$ Mev.

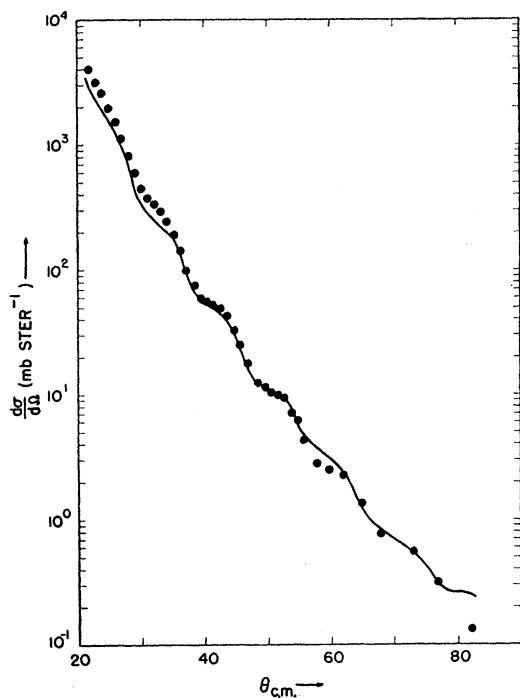


FIG. 8. Angular dependence of the elastic scattering cross section for 40.2-Mev alpha particles scattered from Ag. The dots represent the experimental points; the solid line represents the theoretically predicted distribution for $V_R = -37$ Mev and $V_i = -10$ Mev.

much smaller than that obtained for $d = 0.5 \times 10^{-13}$ cm. The least-square deviation was several hundred times larger than the best fit obtained when $d = 0.5 \times 10^{-13}$ cm.

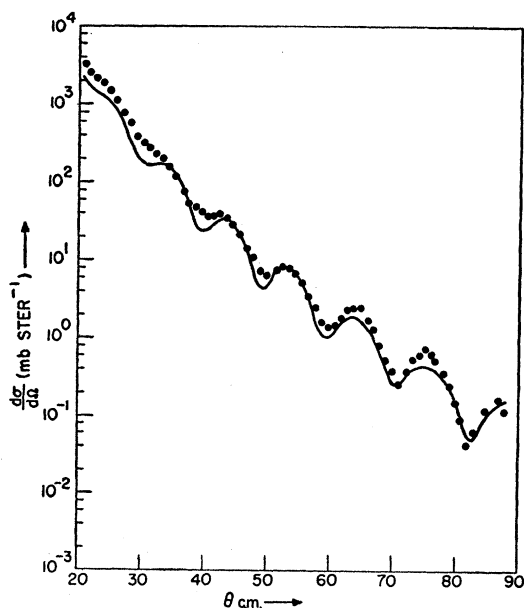


FIG. 9. Angular dependence of the elastic scattering cross section for 40.2-Mev alpha particles scattered from Mo. The dots represent the experimental points; the solid line represents the theoretically predicted distribution for $V_R = -42.5$ Mev and $V_i = -9.5$ Mev.

No minimum was found within the 0 to -100 Mev region when $d = 0.25 \times 10^{-13}$ cm.

The elastic scattering from Cu is typical of the light-element data¹⁶ summarized in Fig. 3. Figure 4 shows the best fit at 40.2 Mev obtained for Cu. The values obtained for the parameters are listed in Table I. The radius was varied in order to test the sensitivity of the

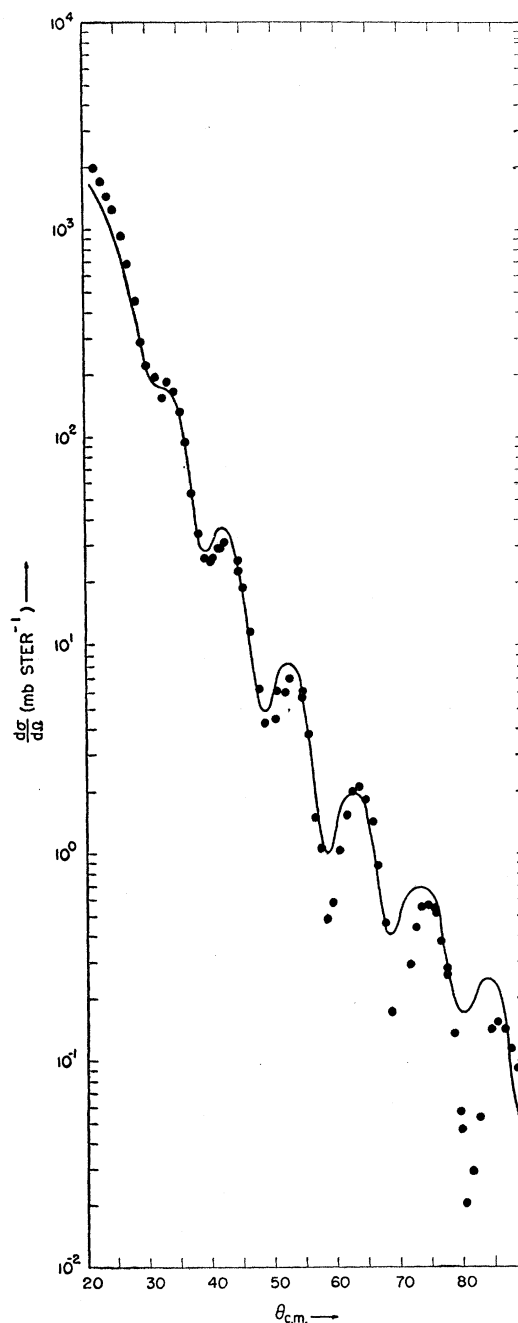


FIG. 10. Angular dependence of the elastic scattering cross section for 40.2-Mev alpha particles scattered from Nb. The dots represent the experimental points; the solid line represents the theoretically predicted distribution for $V_R = -45$ Mev and $V_i = -13.5$ Mev.

fit to nuclear radius. The best fit obtained was for $R = (6.7 \pm 0.3) \times 10^{-13}$ cm $= (1.35A^{\frac{1}{3}} + 1.3) \times 10^{-13}$ cm. The uncertainty in the parameters is taken to be that variation which increases the sum of the least-squares deviation by a factor of two over the minimum value. For several different values of R , the values of V_R and V_i were varied to find the best fit as determined by the minimum in the least squares sum. The position of the minimum in the V_R, V_i space did not vary appreciably for different values of R . This is in contrast to the elastic-proton scattering analysis.³ There it is found that when R is decreased from $R = (1.44A^{\frac{1}{3}}) \times 10^{-13}$ cm to $R = (1.21A^{\frac{1}{3}}) \times 10^{-13}$ cm, equally good fits can be obtained provided V_R and V_i have very different values from before. The values of the parameters for Pb (Fig. 5), Au (Fig. 6), Ta (Fig. 7), Ag (Fig. 8), Mo (Fig. 9), Nb (Fig. 10) are listed in Table I. Figure 11 shows the best fit obtained for Ti, and the values of the parameters obtained are listed in Table I.

A recent analysis of 14-Mev-neutron data¹⁷ has been performed using an imaginary potential more localized on the surface than the real part. However, it is not clear that the 14-Mev neutron data necessarily imply such a potential, since equally good fits are obtained through the use of a potential of the same form as the

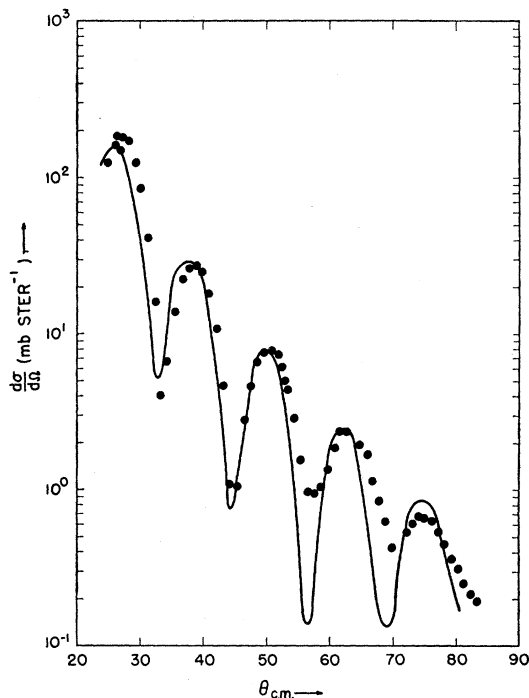


FIG. 11. Angular dependence of the elastic scattering cross section for 40.2-Mev alpha particles scattered from Ti. The dots represent the experimental points; the solid line represents the theoretically predicted distribution for $V_R = -30$ Mev and $V_i = -14$ Mev.

¹⁷ Bjorklund, Fernbach, and Sherman, Phys. Rev. **101**, 1832 (1956).

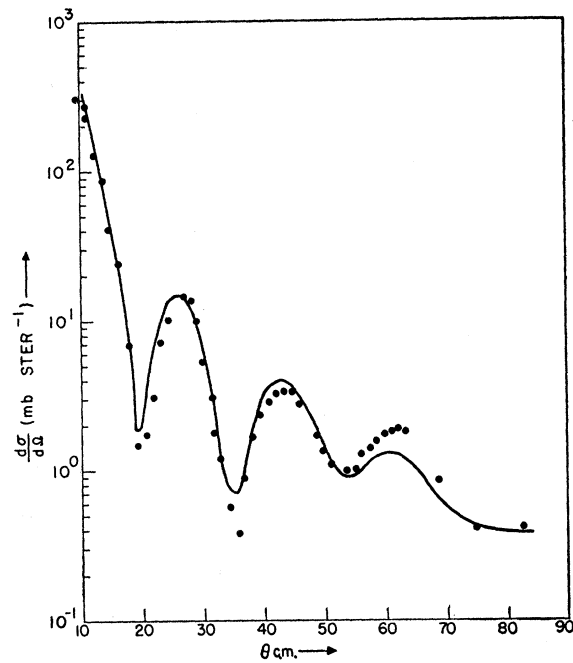


FIG. 12. Angular dependence of the elastic scattering cross section for 40.2-Mev alpha particles scattered from C. The dots represent the experimental points; the solid line represents the theoretically predicted distribution for $V_R = -34$ Mev and $V_i = -10$ Mev.

one assumed here.¹⁸ In order to establish whether better fits could be obtained in the alpha-particle analysis, by using a potential localized on the nuclear surface, the following form for the nuclear potential was also tried in the Ti analysis, *viz.*:

$$V_N = \frac{V_R + irV_i}{1 + \exp[(r - r_1)/d]}$$

The fits obtained were not as good as those obtained for a Fermi function for both real and imaginary parts. These results are not conclusive on this point, however, because the fits were not significantly worse, and because other form factors have not been investigated. Further work is now in progress relating to this question.

A significantly smaller value for V_R , *viz.* $V_R = -30$ Mev, was required to obtain a fit to the Ti data. The same result was found in the analysis of the other two light elements, C (Fig. 12) and Al (Fig. 13).

The results of an analysis of the elastic scattering of 22-Mev alpha particles⁷ on Ag (Fig. 14), Au (Fig. 15), and Pb (Fig. 16) are summarized in Table I.

IV. CONCLUSIONS

The results of an analysis of the elastic scattering of 40-Mev alpha particles from Cu, Nb, Mo, Ag, Ta, Au,

¹⁸ J. R. Beyster, Los Alamos Scientific Laboratory (private communication).

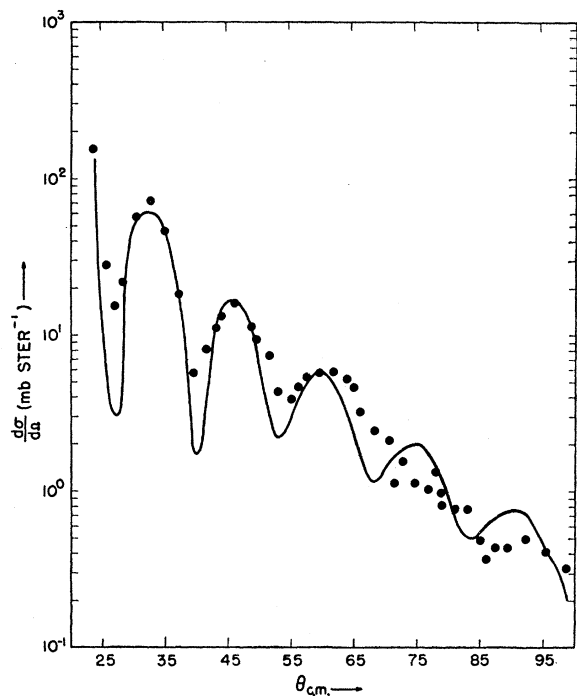


FIG. 13. Angular dependence of the elastic scattering cross section for 40.2-Mev alpha particles scattered from Al. The dots represent the experimental points; the solid line represents the theoretically predicted distribution for $V_R = -30$ Mev and $V_i = -12$ Mev.

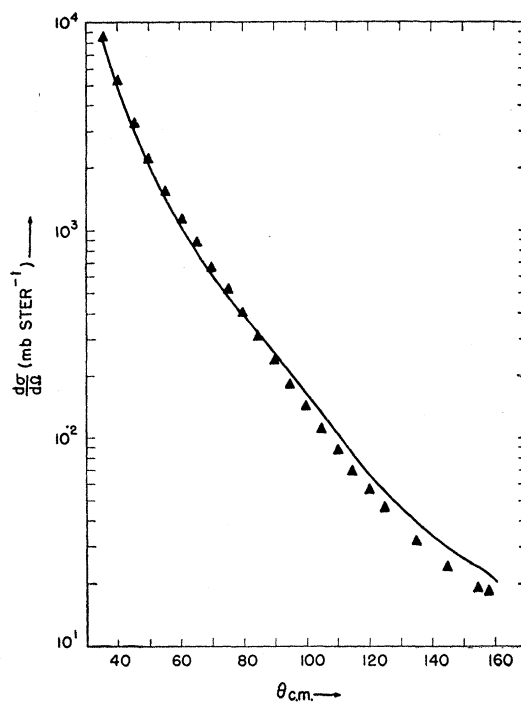


FIG. 15. Angular dependence of the elastic scattering cross section for 20-Mev alpha particles scattered from Au. The dots represent the experimental points; the solid line represents the theoretically predicted distribution for $V_R = -30$ Mev and $V_i = -9.5$ Mev.

Pb, and Th yield a value of (-45_{-7}^{+6}) Mev for V_R , where the deviations represent the maximum excursions

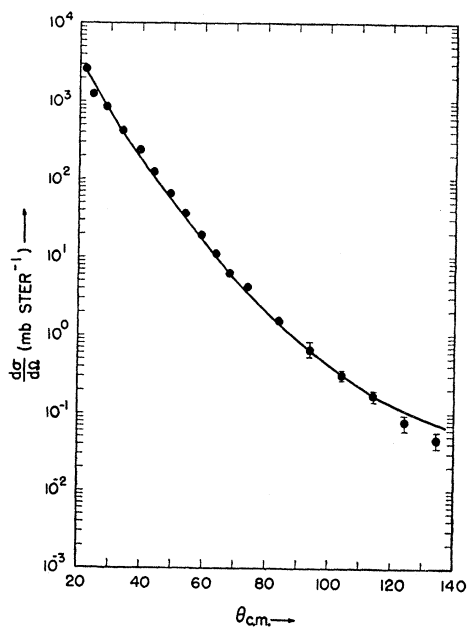


FIG. 14. Angular dependence of the elastic scattering cross section for 20-Mev alpha particles scattered from Ag. The dots represent the experimental points; the solid line represents the theoretically predicted distribution for $V_R = -35$ Mev and $V_i = -7.5$ Mev.

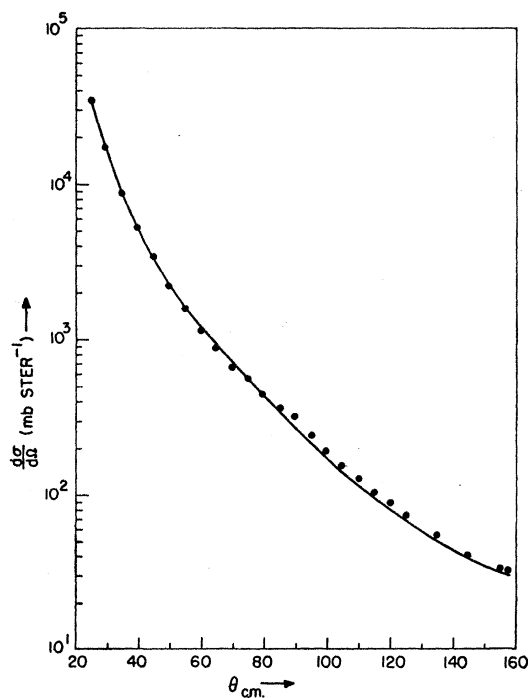


FIG. 16. Angular dependence of the elastic scattering cross section for 20-Mev alpha particles scattered from Pb. The dots represent the experimental points; the solid line represents the theoretically predicted distribution for $V_R = -30$ Mev and $V_i = -17$ Mev.

from -45 Mev among these seven elements. This is in disagreement with the value of -167 Mev obtained by Tolhoek and Brussard¹¹ for the potential experienced by an alpha particle and of -5.6 Mev obtained by Gugelot and Rickey.¹⁹ The value of V_i is $(-10_{-3.5}^{+1.5})$ Mev. The nuclear radius is found to be $R = (1.35A^{\frac{1}{3}} + 1.3) \times 10^{-13}$ cm and the diffuseness parameter $d = 0.5 \times 10^{-13}$ cm.

The three lightest elements investigated at 40 Mev (C, Al, and Ti) compelled the use of a smaller value, -30 Mev, for V_R . A possible explanation of this discrepancy is found in the carbon electron-scattering results.²⁰ They indicate that the charge distribution is approximated better for carbon by a Gaussian than by a Fermi distribution as was used in this analysis for both light and heavy elements. Another reason that V_R may be smaller for light elements is that the energy of the incident 40-Mev alpha particle is appreciably lower in the center-of-mass system for a light element. For a 40-Mev alpha particle incident on C, the center-of mass energy is 30 Mev. That V_R is energy-dependent is indicated by the 22-Mev elastic-scattering analysis.

The mean free path of alpha particles as determined from V_R and V_i obtained in this analysis is $\lambda \cong 2 \times 10^{-13}$

cm at 40 Mev and $\lambda \cong 1.5 \times 10^{-13}$ cm at 22 Mev, where

$$\frac{1}{\lambda^2} = \frac{4\mu}{\hbar^2} (E - V_R) \left\{ \left[\left(\frac{V_i}{E - V_R} \right)^2 + 1 \right]^{\frac{1}{2}} - 1 \right\}.$$

The quantity μ is the reduced mass and E is the energy in the center-of-mass system.

As was mentioned in the discussion of the Ti analysis, the best fit obtained with a Fermi distribution was not a great deal better than that obtained using a surface distribution for V_i . This can be easily understood since the mean-free path is short enough so that the alpha-particle scattering is not particularly sensitive to the central part of the potential. The mean free path of a 40-Mev alpha particle is 2×10^{-13} cm, approximately one-third the interaction radius obtained for Ti. Consequently the alpha particle is absorbed strongly in the outside part of the Ti nucleus, and the analysis is not very sensitive to the central part of the potential.

For comparison, the mean free path for a 20-Mev proton¹ is 3×10^{-13} cm and for a 22-Mev alpha, 1.5×10^{-13} cm from the present analysis. The fact that these mean free paths are not very different is of course a consequence of the fact that the values for V_R and V_i obtained in both analyses are approximately equal. The values for the other parameters are also quite similar in this analysis and in the proton analysis.²

¹⁹ P. C. Gugelot and M. Rickey, *Phys. Rev.* **101**, 1613 (1956).

²⁰ J. H. Fregeau, *Phys. Rev.* **104**, 225 (1956).